Available online at www.sciencedirect.com
ScienceDirect
Bioelectrochemistry 71 (2007) 157–163
Bioelectrochemistry
www.elsevier.com/locate/bioelechem

Study of the adsorption and oxidation of antioxidant rutin by cyclic voltammetry–voltabsorptometry

Jian-Bo He [a,b,*], Yan Wang [a], Ning Deng [a], Xiang-Qin Lin [b]

[a] *Engineering Research Centre for Bio-process, Ministry of Education of China, Hefei University of Technology, Hefei 230009, PR China*
[b] *Department of Chemistry, University of Science and Technology of China, Hefei 230026, PR China*

Received 23 August 2006; received in revised form 15 February 2007; accepted 12 March 2007
Available online 24 March 2007

Abstract

The adsorption and oxidation behavior of rutin was studied by in-situ UV spectroelectrochemistry in a long optical-path thin-layer electrochemical cell with a graphite-wax electrode. The dynamic UV spectra of rutin under potentiostatic oxidation were recorded, which indicated the formation of *o*-quinonic structure. During the repetitive cyclic potential scans, cyclic voltabsorptomogram was recorded at the three characteristic wavelengths 346, 254 and 296 nm, respectively. The profiles obtained showed two types of concentration fluctuation of species in solution, resulting from adsorption/desorption and redox reaction, respectively. Using derivative cyclic voltabsorptometry the contribution of the species in solution to the total current was estimated, and then the current of every step involved in the proposed redox mechanism was obtained for the first time. The result shows that rutin underwent a nearly reversible redox reaction in which the total current is mostly due to the contribution of adsorbed species. The present work developed cyclic voltabsorptometry into a useful tool for investigating redox process involving coupled adsorption/desorption steps.

Keywords: Rutin; Spectroelectrochemistry; Cyclic voltammetry; Cyclic voltabsorptometry; Antioxidant

1. Introduction

Flavonoids, a large group of naturally occurring polyphenols, are widely distributed in plants, fruits, and vegetables and are important constituents of the human diet. The oxidation of flavonoids is of great interest because of their action as antioxidants with the ability to scavenge superfluous superoxide free radicals in human body [1,2] by means of electron-transfer processes. Owing to the antioxidant ability, they can prevent DNA and cells from oxidative damage [3], and then possess a wide range of pharmacological activities such as antitumor, anti-inflammatory and antiaging, etc. Rutin (Scheme 1) is one of the most abundant flavonoids in the human diet. Up to the present, rutin has been used clinically as the therapeutical medicine [4,5], and over 130 preparations containing quercetin or rutin are registered as drugs worldwide [6].

Electrochemical methodologies have been widely used for investigating flavonoids mainly on oxidation mechanism [7–10], electrochemical determination [11,12], metal-chelating properties [13], interaction with DNA [14], evaluation of antioxidant capacity [15], and superoxide-scavenging ability [16], etc. Brett and her co-workers detailedly studied the oxidation mechanism of rutin [8], quercetin [9] and catechin [10] using various voltammetries, and discovered that all these flavonoids and their oxidation products can adsorbs strongly on the electrode surface. From this it can be known that adsorption probably plays an important role for the oxidation activity of flavonoids, which attracts us to explore the contribution of adsorbed species to the total redox current. However, it is difficult experimentally to distinguish between the signals from adsorbed species and from the same species in solution. In theory it also has to be assumed that the rate of reaction of adsorbed species is much greater than of species in solution because of the mathematical difficulty.

* Corresponding author. Engineering Research Centre for Bio-process, Ministry of Education of China, Hefei University of Technology, Hefei 230009, PR China. Tel.: +86 551 2901450; fax: +86 551 2901450.
E-mail address: jbhe@hfut.edu.cn (J.-B. He).

1567-5394/$ - see front matter © 2007 Elsevier B.V. All rights reserved.
doi:10.1016/j.bioelechem.2007.03.003

The combination of cyclic voltammetry and spectrophotometry offers the possibility of recording simultaneously the changes in current and absorbance with potential [17,18]. The latter can reflect the change in concentration of the species in solution. Based on this it is possible to subtract the contribution of the species in solution from the total current. For this objective the multi-cycle cyclic voltabsorptomograms were recorded at three characteristic wavelengths of rutin in a simple and reliable long optical-path thin-layer electrochemical cell. A graphite-wax electrode (GWE) was used as working electrode because the carbon-wax electrode has advantages of low background currents, low noise and fast base line stabilization [19]. Using derivative cyclic voltabsorptometry [17], the contribution of the species in solution to the total current was estimated, and then the current of every step involved in the proposed redox mechanism was obtained for the first time.

2. Experimental

2.1. Chemicals and solutions

Rutin is reagent-grade materials from Shanghai Chemical Works (Shanghai China). Spectrograde graphite powder (320 meshes, Shanghai Chemical Works) was used for construction of GWE. Doubly-distilled water from an all-glass distillatory apparatus was used. High pure N_2 was used for solution deaeration. All other chemicals were of analytical grade from Shanghai Chemical Works (Shanghai China).

The 0.2 M Britton-Robinson buffered solutions (BRS) containing 0.5 M KCl with various pH values were prepared as the supporting electrolytes. With the aid of ultrasonication, 1.0 mM stock solution of rutin was prepared with ethanol, and stored at 4 °C in a refrigerator before used. Before used it was diluted to various convenient concentrations by mixing with buffer supporting electrolyte.

2.2. Apparatus

UV–Vis absorption spectra and kinetic curves were measured using a model UV-2500 spectrophotometer with UV probe data software (Shimadzu, Japan).

Electrochemical measurements were carried out on a model CHI 660 microcomputer-based electrochemical analyzer (CHENHUA, Shanghai, China). Three-electrode system was used, which is consisted of a graphite-wax disk working electrode (GWE), a platinum grid counter electrode, and a Ag/AgCl/KCl_{sat} reference electrode.

2.3. Cell design

A long-path length thin layer UV–Vis spectroelectrochemical cell (shorted as SE-cell) was constructed as shown in Fig. 1. The cell was a commercial available quartz photometric cell (1) with an optical path length of 10 mm, containing three electrode system. A graphite-wax plate working electrode was used, the detailed structure of which is shown in Fig. 1B. Dry graphite powder and pre-molten wax were mixed (5:2 w/w) thoroughly in an agate mortar, then crammed into the quadrate hollow space (8 mm × 9.6 mm) on a polyethylene strip plate (2) and led out with an embedded copper foil (3). The GWE was polished to a flat surface with emery papers and then covered with a PTFE plate (4), on which 9 holes of 0.1 mm diameter (5) were drilled symmetrically against the GWE. The slit (6) of 0.2 mm for light path was formed using two spacers (7). The surface area of the GWE and the thin-layer solution can be estimated as 77 mm^2 and 16 μL, respectively. A counter electrode (8) was placed in the cell outside the PTFE plate (4), and led out the electrolysis current from the GWE through the holes on the PTFE plate. The reference electrode (9) was placed in the other side of solution (referred as the reference chamber), which was connected to the thin-layer solution through a small slot (10) lies on the side edge of the GWE.

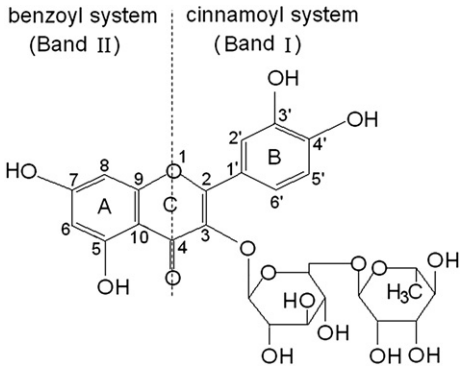

Scheme 1. Molecular structure of rutin.

2.4. Procedure

Before experiment, the electrochemical cell was washed with water and ethanol successively for 1 min under ultrasonication. All the experiments were carried out at room temperature (22 ± 1 °C).

Rutin solutions were bubbled with N_2 for about 15 min to remove dissolved oxygen before put into the cell. The GWE was degreased with ethanol for 3 min and then washed with water before each measurement.

For spectroelectrochemical experiment, a 1.0-ml portion of rutin solution was injected into the SE-cell through the thin-layer chamber and then infiltrated into the two side chambers, ensuring no gas bubble in the thin layer compartment. An in-situ UV–Vis absorption spectrum was measured during the thin-layer solution was electrolyzed at a steady potential. On the other hand, kinetic absorbance monitoring coupled with CV scans were taken at certain wavelengths to follow the concentration changes of species in the thin layer solution.

Considering the strong adsorption of rutin on GWE, a pre-accumulation step was always performed in open circuit. The accumulation time of 400 s was used in this work.

3. Results and discussion

3.1. Thin-layer behavior of the spectroelectrochemical cell

The performance of the thin layer cell was tested by obtaining cyclic voltammogram (CV) of a known reversible redox couple.

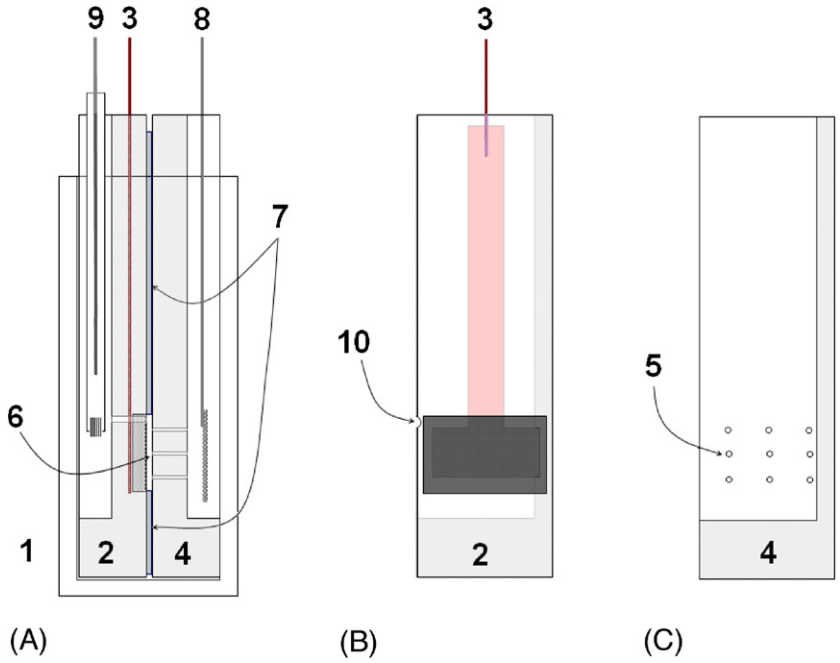

Fig. 1. Long optical-path thin layer spectroelectrochemical cell. (A) Front view of the cell; (B) Side view of the GWE and (C) Side view of the PTFE counter plate: (1) 1-cm quartz cell; (2) GWE plate; (3) copper foil lead; (4) PTFE counter plate; (5) current channels (Φ 0.1 mm) on the plate; (6) slit for light path; (7) thin-layer spacers (0.2 mm thickness); (8) Pt grid counter electrode; (9) Ag/AgCl/KCl_{sat} reference electrode; (10) reference channel.

Fig. 2A illustrates a multi-circle CV profile recorded in a aqueous solution of 1 mM $Fe(CN)_6^{3-/4-}$ plus 1.0 M KCl. The peak-to-peak separation, ΔE_p, is 43 mV at a scan rate of 1 mV s^{-1}. This small value of ΔE_p, less than the 57 mV expected for the $1e^-$ process in the bulk CV experiment, indicates that even at the relatively large layer thickness (0.2 mm), the cell shows characteristics tending toward the theoretical value (ΔE_p=0 mV) predicted for a thin layer. Small edge effects were present as shown by the fact that the current largely approached the baseline after electro-reduction. Fig. 2B was the cyclic voltabsorptomogram (CVA) recorded simultaneously with Fig. 2A; it shows the typical variation of absorbance with potential in a thin layer cell. The characteristics of exhaustive electrolysis can be seen in Fig. 2B – the below horizontal line means that the electroactive species has fully transformed to its reduced form, $K_4Fe(CN)_6$, and the above to its oxidized form, $K_3Fe(CN)_6$. Comparison of Fig. 2B with Fig. 2A clarifies real-time response of absorbance to concentration variation of the species in the thin layer during the electrode process.

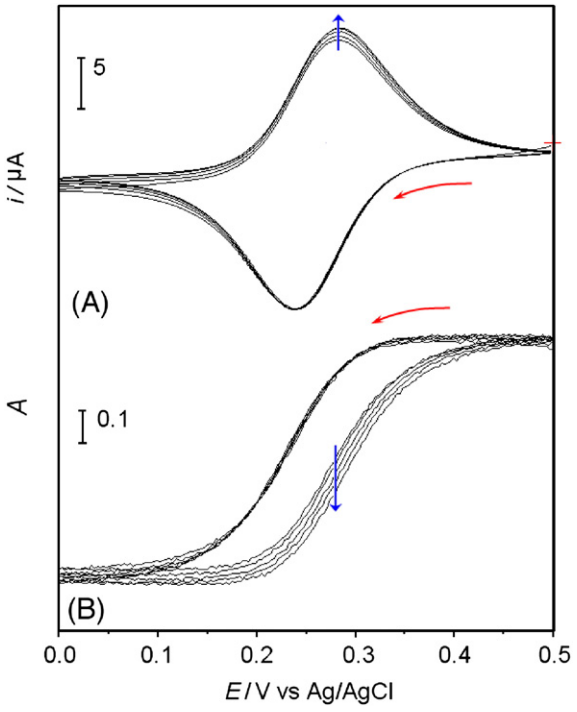

Fig. 2. Multi-cycle thin layer CV (A) and CVA (B) of 1 mM $K_3Fe(CN)_6$.in the SE-cell with a GWE working electrode. Supporting electrolyte: 1.0 M KCl; scan rate: 1 mV s^{-1}; wavelength: 420 nm.

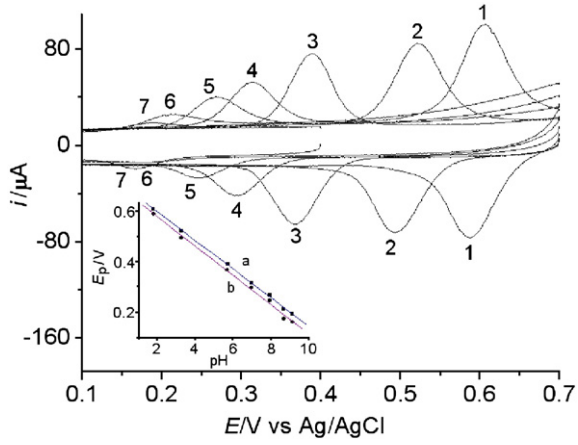

Fig. 3. CVs of 10 μM rutin recorded at scan rate 100 mV s^{-1}. pH: (1) 1.8; (2) 3.3; (3) 5.7; (4) 7.0; (5) 8.0; (6) 8.7; (7) 9.2. Inset: pH-dependencies of peak potentials of A1 (a) and its counterpart peak C1 (b).

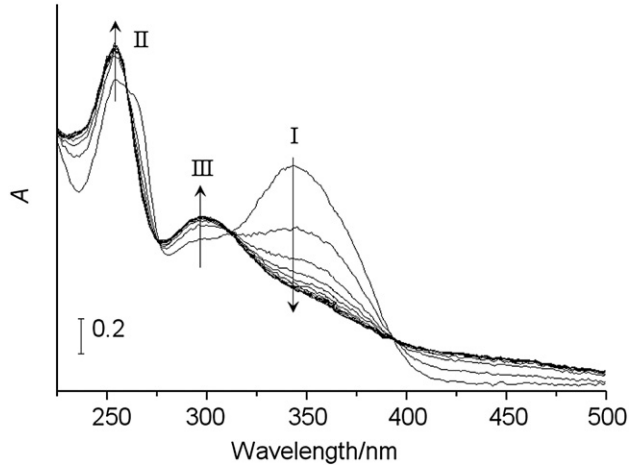

Fig. 4. Thin-layer UV absorption spectra of rutin during potentiostatic oxidation at 0.60 V in 0.1 mM rutin (pH 1.8). Spectral tracing was repeated every 50 s after the potential was applied. The first line was recorded before electrolysis.

3.2. Adsorption characteristic of CV peaks

The CVs of rutin (Ru) were recorded in a conventional cell with the GWE working electrode, as shown in Fig. 3. A couple of well-shaped CV peaks A1/C1 appeared corresponding to the redox of the 3′,4′-dihydroxyl groups at B-ring of rutin [8,11]. The slope of peak potentials (E_p) vs. pH was found to be −57 mV/pH for A1 and −58 mV/pH for C1 (Fig. 3, inset), respectively, indicating an equal number of electron and proton involved. At the same time the currents of both the peaks decreased obviously with the increase of pH. Since acidic medium is advantageous to the oxidation of rutin, pH 1.8 was selected for the following investigation.

It is worth while to discuss the small peak-to-peak separation (ΔE_p) of A1/C1 couple. For example, ΔE_p was only 18 mV when pH=1.8. This separation decreased further with the decrease in scan rate. At scan rate of 5 mV s^{-1} ΔE_p was as small as 7 mV. Such a small ΔE_p in a conventional cell suggests a couple of nearly reversible adsorption waves [20]. The adsorption of rutin on the GWE was also demonstrated by measuring the absorbance of the thin-layer solution in open circuit — the absorbance decreased with time until approaching a stable value. About 400 s was needed for adsorption equilibrium in open circuit, so a pre-accumulation time of 400 s was used in this work.

3.3. Dynamic UV spectra at constant potential

The thin layer UV–Vis spectra of rutin (0.1 mM, pH 1.8) were measured repeatedly before and during controlled-potential electrolysis at 0.60 V to investigate the oxidation process in peak A1 (Fig. 4). Rutin exhibits two characteristic absorption bands of flavonoid compounds at 346 nm (band I) and 254 nm (band II), along with a very weak band at 296 nm (band III). By means of theoretical investigation of the molecular structure, band I of flavonoids was considered to be primarily due to the HOMO-LUMO transition, for which the electronic charge density is mainly withdrawn from the B-ring to C(4)=O bond [21]. It is well-known that the band I of flavonoids corresponds to the B-ring portion (cinnamoyl system) and band II corresponds to A-ring portion (benzoyl system) (Scheme 1) [22]. In addition, hydroxyl groups at the carbon rings have more or less influence on these two characteristic bands in both intensity and location, depending on the position and number of hydroxyl groups. As for band III few reports and analyses are available, since it is either absent or considerably diminished in intensity for many flavonoids. Presumably the band III may be related to the keto-hydroxyl tautomerism between 4- and 7-positions of rutin molecule, leading to a quinonic resonant structure as suggested for quercetin [23].

Fig. 4 shows that band I of rutin decreased largely during electro-oxidation at 0.60 V, simultaneous with a few rise of bands II and III. It is well known that the 3′,4′-OH groups at B-ring can enhance band I but weaken band II. Contrarily, the OH groups at A-ring (especially 5-OH) usually intensify band II and weaken band I. For a flavonoid compound with OH groups only at A-ring, band I is generally a very weak shoulder peak. Therefore, the spectral change shown in Fig. 4 supports the carbonylation of the 3′,4′-OH groups at B-ring, which causes the loss of the electron donating ability of B-ring. In addition, band II of rutin is a superposed double-peaks (Fig. 4, the first line), due to the effect of 3′,4′-OHs at B-ring. It became a single peak after subjected to the electro-oxidation, also suggesting the

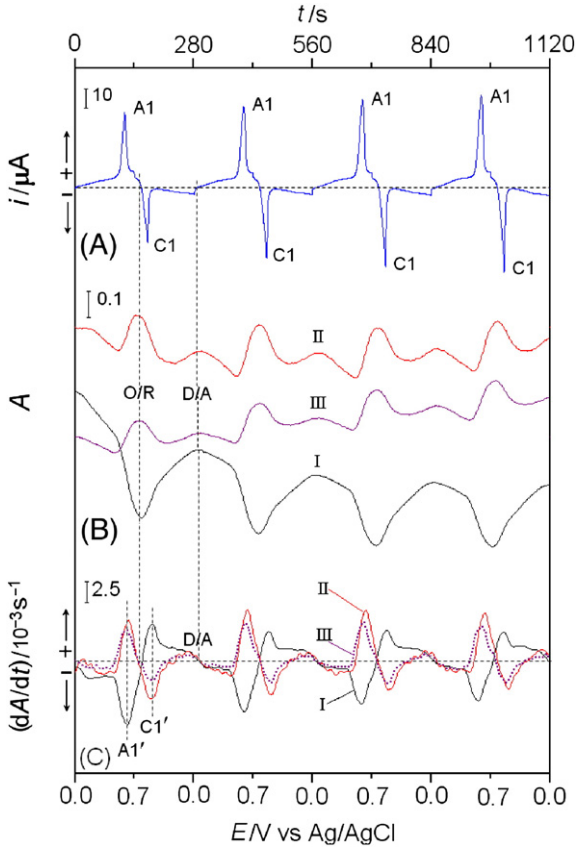

Fig. 5. Multi-cycle thin layer CVs (A) and CVAs (B) and DCVAs (C) of 0.1 mM rutin (pH=1.8). Scan rate: 5 mV s^{-1}; wavelength: (I) 346 nm, (II) 254 nm, (III) 296 nm.

Table 1
Current of each step in rutin redox mechanism during 4-cycle CV scan (original data from Fig. 5)

Step	Current type	Current value (μA)			
		1[a]	2	3	4
(1)	$i_{ad,(1)}$[b]	0.21	0.17	0.18	0.20
(2)	$i_{p,ad,(2)}$	27.7	31.3	34.4	36.8
(3)	$i_{p,dif,(3)}$	2.52	2.19	1.92	1.81
(4)	$i_{p,dif,(4)}$	2.91	2.79	2.54	2.40
(5)	$i_{p,ad,(5)}$	−26.0	−34.1	−38.8	−41.1
(6)	$i_{p,dif,(6)}$	−2.04	−1.72	−1.62	−1.56
(7)	$i_{p,dif,(7)}$	−1.60	−1.31	−1.30	−1.24
(8)	$i_{ad,(8)}$[c]	−0.18	−0.17	−0.18	−0.19

[a]The number of cycling, n_{cyc}.
[b, c]The rate of adsorption or desorption (see Eq. (2)), expressed in current form.

variation of 3′,4′-OH groups at B-ring. The carbonylation of 3′,4′-OHs was probably favorable to the quinonic resonant structure, leading to stronger absorbance in band III.

In the following investigation, the absorbances at all three bands (A_{346}, A_{254} and A_{296}) were utilized to follow the change in concentration of Ru and its oxidation product RuQ in the thin layer solution during the cyclic potential scan.

3.4. Thin-layer cyclic voltammetry–voltabsorptometry

During the repetitive CV scans between 0.0 and 0.7 V the CVAs were recorded at three wavelengths, 346 nm, 254 nm and 296 nm, respectively, as shown in Fig. 5B along with the corresponding CV in Fig. 5A for comparison. Whichever wavelength was set, the absorbances presented two periodical waves within one circle of scan. One of the waves, which was marked with sign "O/R", corresponded to the anodic switching of scan. In the left branch of wave O/R, A_{346} decreased at relatively fast rates whereas A_{254} and A_{296} increased, indicating the decrease of rutin and the increase of product (RuQ) in the thin layer due to the oxidation reaction in peak A1. The contrary changes in absorbances occurred in the right branch of wave O/R, associated with the reduction of RuQ in peak C1.

Another absorbance wave, marked with sign "D/A", occurred synchronously with the cathodic switching of scan. No CV peak appeared in this potential range, so the wave D/A can be attributed to the effect of potential on the adsorption/desorption phenomenon. After regenerated in peak C1, rutin was driven away from the electrode surface into the thin layer by interfacial electric field with the potential negative-going, and re-adsorbed onto electrode after the potential was reversed. This Desorption/Adsorption step led to the increase and decrease in absorbance at all three wavelengths before and after the cathodic switching of potential, respectively.

On the basis of above analysis, it is clear that both the pre-adsorbed species and those in solution were involved in the reactions of peaks A1 and C1, via the adsorption/desorption steps in series with the electron transfer step. The interfacial process during CV scan may be described as follows:

$$\mathrm{Ru_{sol}} \xrightarrow[A_{254,296,346}\downarrow]{(1)\ \text{adsorption}} \mathrm{Ru_{ad}} \qquad \text{prior to peak A1}$$

$$\left.\begin{array}{l} \mathrm{Ru_{ad}} \xrightarrow{(2)-2H^+-2e^-} \mathrm{RuQ_{ad}} \\ \mathrm{Ru_{sol}} \xrightarrow[A_{254,296,346}\downarrow]{(3)-2H^+-2e^-} \mathrm{RuQ_{ad}} \end{array}\right\} \xrightarrow[A_{254,296,346}\uparrow]{(4)\text{desorption}} \mathrm{RuQ_{sol}} \text{ at A1}$$

$$\left.\begin{array}{l} \mathrm{RuQ_{ad}} \xrightarrow{(5)+2H^++2e^-} \mathrm{Ru_{ad}} \\ \mathrm{RuQ_{sol}} \xrightarrow[A_{254,296,346}\downarrow]{(6)+2H^++2e^-} \mathrm{Ru_{ad}} \end{array}\right\} \xrightarrow[A_{254,296,346}\uparrow]{(7)\text{desorption}} \mathrm{Ru_{sol}} \text{ at C1}$$

$$\mathrm{Ru_{ad}} \xrightarrow[A_{254,296,346}\uparrow]{(8)\text{desorption}} \mathrm{Ru_{sol}} \qquad \text{after peak C1}$$

From the Lambert–Beer's law it can be known that the change of absorbance (A) is proportional to that of volume concentration (c) of species in solution:

$$\frac{\mathrm{d}A}{\mathrm{d}t} = \varepsilon l \frac{\mathrm{d}c}{\mathrm{d}t} \tag{1}$$

where ε is the molar extinction coefficient at characteristic wavelength, l is the pathlength of the light through the solution.

For the pure adsorption and desorption steps (1) and (8) of Ru, we can deduce the rate of adsorption/desorption under the action of potential scan:

$$\frac{\mathrm{d}\Gamma_{\mathrm{Ru}}}{\mathrm{d}t} = -V\frac{\mathrm{d}c_{\mathrm{Ru}}}{\mathrm{d}t} = -\frac{V}{\varepsilon_{\mathrm{Ru}} l}\frac{\mathrm{d}A}{\mathrm{d}t} \tag{2}$$

where Γ_{Ru} is the extent of adsorption of Ru on the surface of electrode, V is the cell volume. In order to obtain the derivative of absorbance A with respect to time t, the corresponding derivative cyclic voltabsorptomogram (DCVA) was computed from the CVA data in Fig. 5B, as shown in Fig. 5C, which shows an excellent agreement with the CV data in Fig. 5A. In the potential ranges where adsorption step (1) or desorption step (8) occurred, the DCVAs showed roughly a negative or positive plateau, respectively. Here $\mathrm{d}\Gamma_{\mathrm{Ru}}/\mathrm{d}t$ was estimated from the $\mathrm{d}A_{296}/\mathrm{d}t$ plateau value via Eq. (2) by putting $V = 16$ μL, $l = 1$ cm, $\varepsilon_{296}(\mathrm{Ru}) = 1.046 \times 10^7$ cm^2 mol^{-1} (All ε values in this work are from experiment). By a transformation using the Faraday's law, the result was expressed in current form (see Table 1), $i_{ad,(1)}$ and $i_{ad,(8)}$, for comparison with the rate of other steps.

Each profile in Fig. 5C presents two differentiated waves, A1′ and C1′, corresponding to the CV peaks A1 and C1, respectively. Both pre-adsorbed species and those in solution contribute to the total current in these two peaks. The adsorption contribution results from steps (2) and (5) while that of diffusion is from steps (3) and (6). The latter is possible to be estimated from the differentiated waves. Because both Ru and its product RuQ in solution contribute to the absorption at three characteristic bands (see Fig. 4), the superposition of signal should be considered. At wavelength 346 nm and 254 nm, respectively, we have

$$\frac{\mathrm{d}A_{346}}{\mathrm{d}t} = \varepsilon_{346,\mathrm{Ru}} l \frac{\mathrm{d}c_{\mathrm{Ru}}}{\mathrm{d}t} + \varepsilon_{346,\mathrm{RuQ}} l \frac{\mathrm{d}c_{\mathrm{RuQ}}}{\mathrm{d}t} \tag{3}$$

$$\frac{\mathrm{d}A_{254}}{\mathrm{d}t} = \varepsilon_{254,\mathrm{Ru}} l \frac{\mathrm{d}c_{\mathrm{Ru}}}{\mathrm{d}t} + \varepsilon_{254,\mathrm{RuQ}} l \frac{\mathrm{d}c_{\mathrm{RuQ}}}{\mathrm{d}t} \tag{4}$$

By solving these simultaneous equations we get

$$\frac{dc_{Ru}}{dt} = \frac{\varepsilon_{346,RuQ}}{l\Delta\varepsilon\varepsilon}\frac{dA_{254}}{dt} - \frac{\varepsilon_{254,RuQ}}{l\Delta\varepsilon\varepsilon}\frac{dA_{346}}{dt} \quad (5)$$

$$\frac{dc_{RuQ}}{dt} = \frac{\varepsilon_{254,Ru}}{l\Delta\varepsilon\varepsilon}\frac{dA_{346}}{dt} - \frac{\varepsilon_{346,Ru}}{l\Delta\varepsilon\varepsilon}\frac{dA_{254}}{dt} \quad (6)$$

where $\Delta\varepsilon\varepsilon = \varepsilon_{346,RuQ}\varepsilon_{254,Ru} - \varepsilon_{346,Ru}\varepsilon_{254,RuQ}$, in which $\varepsilon_{346,Ru} = 1.663\times10^7$ cm^2 mol^{-1}, $\varepsilon_{254,Ru} = 1.982\times10^7$ cm^2 mol^{-1}, $\varepsilon_{346,RuQ} = 0.645\times10^7$ cm^2 mol^{-1} and $\varepsilon_{254,RuQ} = 2.225\times10^7$ cm^2 mol^{-1}. Combining Eqs. (5) and (6) with the Faraday's law [24] leads to

$$i_{dif,(3)/(7)} = -zFV\left(\frac{\varepsilon_{346,RuQ}}{l\Delta\varepsilon\varepsilon}\frac{dA_{254}}{dt} - \frac{\varepsilon_{254,RuQ}}{l\Delta\varepsilon\varepsilon}\frac{dA_{346}}{dt}\right) \quad (7)$$

$$i_{dif,(4)/(6)} = zFV\left(\frac{\varepsilon_{254,Ru}}{l\Delta\varepsilon\varepsilon}\frac{dA_{346}}{dt} - \frac{\varepsilon_{346,Ru}}{l\Delta\varepsilon\varepsilon}\frac{dA_{254}}{dt}\right) \quad (8)$$

where $i_{dif,(3)/(7)}$ is the diffusion contribution from step (3) or (7), $i_{dif,(4)/(6)}$ is that from step (4) or (6), other symbols have their usual meanings.

Reading the peak values of differentiated waves A1′ and C1′ in the DCVAs, $(dA_{346}/dt)_p$ and $(dA_{254}/dt)_p$, and substituting in Eqs. (7) and (8), we obtain the peak currents of steps (3), (4), (6) and (7), $i_{p,dif,(j)}$ (j=3, 4, 6, 7), respectively. On the other hand, the peak current of adsorption reaction (2), $i_{p,ad,(2)}$, can be obtained by subtracting that of step (3), $i_{p,dif,(3)}$, from the total peak current i_p(A1) (after background correction) in Fig. 5A. Also, for adsorption reaction (5), $i_{p,ad,(5)} = i_p(C1) - i_{p,dif,(6)}$. Results are also listed in Table 1, from which we can know:

- $i_{p,ad,(2)} \gg i_{p,dif,(3)}$, $i_{p,ad,(5)} \gg i_{p,dif,(6)}$, that is, the contribution of adsorbed species to the total current was much greater than that of the species in solution, whether oxidation in peak A1 or reduction in peak C1. This is consistent with the fact that the CV of rutin in a conventional cell exhibited the characteristic of adsorption wave, as discussed in Section 3.2.
- The diffusion contribution ($i_{p,dif,(3)}$ and $i_{p,dif,(6)}$) decreased with the number of cycling, n_{cyc}, therefore, the increase of the total current (i_p(A1) and i_p(C1)) with n_{cyc} was due to the increase of the adsorption contribution ($i_{p,ad,(2)}$ and $i_{p,ad,(5)}$).
- $i_{p,dif,(6)} < i_{p,dif,(4)}$ suggests that the oxidation product RuQ in solution could not be reduced completely at peak C1. Thus, RuQ_{sol} accumulated slowly in solution with the increase of n_{cyc}, leading to the slow ascending trend of A_{254} and A_{296} along with the repeated CV scan (see profiles II and III in Fig. 5B). On the other hand, $i_{p,dif,(3)} > i_{p,dif,(7)}$ suggests that the concentration of Ru_{sol} in solution decreased simultaneously.

The thin-layer cyclic voltabsorptometric behavior of rutin was also investigated at faster scan rates. Unexpectedly, during the repeated CV scan both A_{254} vs. $E(t)$ (Fig. 6) and A_{296} vs. $E(t)$ (not shown) presented a minimum at a certain time (about 100 s). The same data processing as described above was made for the profile (a) in Fig. 6. The result obtained definitely reveals the cause of the minimum point. On the initial several cycles of the scan, the rates of desorption steps (4), (7) and (8) were small, leading to the increase in adsorption extent of Ru on the electrode surface with n_{cyc} and then the decrease in absorbance at all three characteristic wavelengths. In other words, because the adsorption rate of Ru could not keep up with the faster scan rate during the positive-going scan, several cycles were needed for equilibrium adsorption. The faster scan rate was, the more cycles were needed. On the other hand, with the increase in adsorption extent of Ru on electrode, the desorption rate of step (4) increased with n_{cyc} (contrary to the change under slower scan shown in Table 1), leading to the accumulation of RuQ in solution and then the increase of both A_{254} and A_{296}. Thus, a minimum point appeared on the profiles of both A_{254} vs. $E(t)$ and A_{296} vs. $E(t)$.

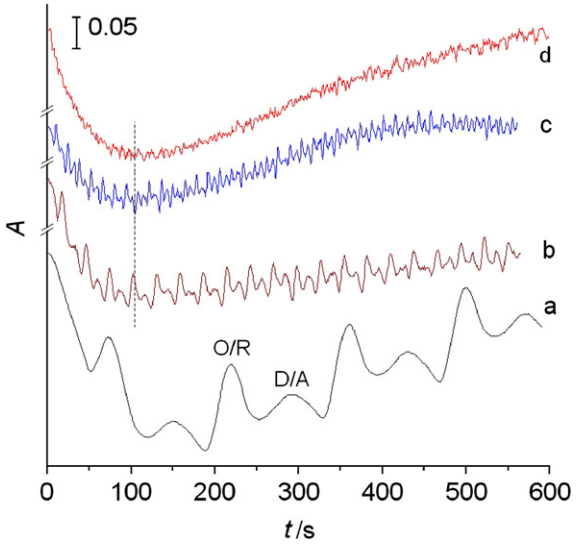

Fig. 6. Chronoabsorptomograms of 0.1 mM rutin (pH=1.8). Potential scan range: 0.0–0.7 V; wavelength 254 nm; scan rate: (a) 10 mV s^{-1}; (b) 50 mV s^{-1}; (c) 100 mV s^{-1}; (d) 500 mV s^{-1}.

4. Conclusions

The adsorption and oxidation of antioxidant rutin has been investigated on a graphite-wax electrode by in-situ thin layer UV spectroelectrochemistry. During the electro-oxidation the absorbance bands of rutin at 346, 254 and 296 nm showed changes in intensity, suggesting the formation of *o*-quinonic structure at catechol moiety. Two types of concentration fluctuation of species in solution, resulting from adsorption/desorption and redox reaction respectively, were observed from the multi-cycle cyclic voltabsorptomograms at three characteristic wavelengths. The contribution of the species in solution to the total current was estimated using derivative cyclic voltabsorptometry, and then the current of every step involved in the proposed redox mechanism was obtained. The result shows that rutin underwent a nearly reversible redox reaction in which the total current is mostly due to the contribution of adsorbed species Ru_{ad} and RuQ_{ad}. In this way, the present work developed cyclic voltabsorptometry into a useful tool for

investigating electrochemical process involving coupled adsorption/desorption steps.

Acknowledgments

The authors gratefully acknowledge financial support from Open Fund of Key Lab for Bio-process, Ministry of Education of China.

References

[1] S. Teixeira, C. Siquet, C. Alves, I. Boal, M.P. Marques, F. Borges, J.L.F.C. Lima, S. Reis, Structure–property studies on the antioxidant activity of flavonoids present in diet, Free Radic. Biol. Med. 39 (2005) 1099–1108.
[2] J. Zhang, R.A. Stanley, A. Adaim, L.D. Melton, M.A. Skinner, Free radical scavenging and cytoprotective activities of phenolic antioxidants, Mol. Nutr. Food Res. 50 (2006) 996–1005.
[3] Ü. Ündeğer, S. Aydın, A.A. Başaran, N. Başaran, The modulating effects of quercetin and rutin on the mitomycin C induced DNA damage, Toxicol. Lett. 151 (2004) 143–149.
[4] W.Q. Sun, J.F. Sheng, Handbook of Natural Active Constituents, Chinese Medicinal Science and Technology Press, Beijing, 1998, pp. 2240–2316.
[5] J.E.F. Reynolds, MARTINDALE, The Extra Pharmacopoeia, The Royal Pharmaceutical Society, Council of the Royal Pharmaceutical Society of Great Britain, London, 1996, pp. 1679–1680.
[6] I. Erlund, T. Kosonen, G. Alfthan, J. Mäenpää, K. Perttunen, J. Kenraali, J. Parantainen, A. Aro, Pharmacokinetics of quercetin from quercetin aglycone and rutin in healthy volunteers, Eur. J. Clin. Pharmacol. 56 (2000) 545–553.
[7] P. Rapta, V. Mišík, A. Staško, I. Vrábel, Redox intermediates of flavonoids and caffeic acid esters from propolis: an EPR spectroscopy and cyclic voltammetry study, Free Radic. Biol. Med. 18 (1995) 901–908.
[8] M.-E. Ghica, A.M.O. Brett, Electrochemical oxidation of rutin, Electroanalysis 17 (2005) 313–318.
[9] A.M.O. Brett, M.-E. Ghica, Electrochemical oxidation of quercetin, Electroanalysis 15 (2003) 1745–1750.
[10] P. Janeiro, A.M.O. Brett, Catechin electrochemical oxidation mechanisms, Anal. Chim. Acta 518 (2004) 109–115.
[11] A.R. Malagutti, V.G. Zuin, E.T.G. Cavalheiro, L.H. Mazo, Determination of rutin in green tea infusions using square-wave voltammetry with a rigid carbon–polyurethane composite electrode, Electroanalysis 18 (2006) 1028–1034.
[12] X.-Q. Lin, J.-B. He, Z.-G. Zha, Simultaneous determination of quercetin and rutin at a multi-wall carbon-nanotube paste electrodes by reversing differential pulse voltammetry, Sens. Actuators, B, Chem. 119 (2006) 608–614.
[13] M.d. Vestergaard, K. Kerman, E. Tamiya, An electrochemical approach for detecting copper-chelating properties of flavonoids using disposable pencil graphite electrodes: Possible implications in copper-mediated illnesses, Anal. Chim. Acta 538 (2005) 273–281.
[14] A.M.O. Brett, V.C. Diculescu, Electrochemical study of quercetin–DNA interactions Part II. In situ sensing with DNA biosensors, Bioelectrochemistry 64 (2004) 143–150.
[15] S. Chevion, M.A. Roberts, M. Chevion, The use of cyclic voltammetry for the evaluation of antioxidant capacity, Free Radic. Biol. Med. 28 (2000) 860.
[16] Y. Wei, X. Ji, X. Dang, Study of electrochemical properties of scavenge of superoxide anion in aprotic media by using carbon nanotubes powder microelectrode, Bioelectrochemistry 61 (2003) 51–56.
[17] E.E. Bancorft, J.S. Sidwell, H.N. Blount, Derivative linear sweep and derivative cyclic voltabsorptometry, Anal. Chem. 53 (1981) 1390–1394.
[18] Y. Astuti, E. Topoglidis, G. Gilardi, J.R. Durrant, Cyclic voltammetry and voltabsorptometry studies of redox proteins immobilised on nanocrystalline tin dioxide electrodes, Bioelectrochemistry 63 (2004) 55–59.
[19] V. Rajendran, E. Csoregi, Y. Okamota, L. Gorton, Amperometric peroxide sensor based on horseradish peroxidase and toluidine blue *o*-acrylamide polymer in carbon paste, Anal. Chim. Acta 373 (1998) 241–251.
[20] C.M.A. Brett, A.M.O. Brett, Electrochemistry: Principles, Methods and Applications, Oxford University Press, Oxford, 1993, pp. 185–187.
[21] J.P. Cornard, A.C. Boudet, J.C. Merlin, Theoretical investigation of the molecular structure of the isoquercitrin molecule, J. Mol. Struct., Theochem 508 (1999) 37–49.
[22] K.R. Markham, Flavones, Flavonols and Their Glycosides, in: J.B. Harborne (Ed.), Methods in Plant Biochemistry, Plant Phenolics, vol. 1, Academic Press, New York, 1989, pp. 197–235.
[23] G. Galati, M.Y. Moridant, T.S. Chan, P.J. O'Brien, Peroxidative metabolism of apigenin and naringenin versus luteolin and quercetin: glutathione oxidation and conjugation, Free Radic. Biol. Med. 30 (2001) 370–382.
[24] J. Agrisuelas, D. Giménez-Romero, J.J. García-Jareño, F. Vicente, Vis/NIR spectroelectrochemical analysis of poly-(Azure A) on ITO electrode, Electrochem. Commun. 8 (2006) 549–553.